

**CELLULOSE NANOCOMPOSITE AS AN EFFECTIVE SUBSTRATE  
FOR ORGANIC LIGHT EMITTING DIODES (OLEDs)**



Sarute Ummartyotin

A Thesis Submitted in Partial Fulfillment of the Requirement for the  
Degree of Doctor of Philosophy  
The Petroleum and Petrochemical College, Chulalongkorn University  
in Academic Partnership with  
The University of Michigan, The University of Oklahoma,  
and Case Western Reserve University

2012

551763

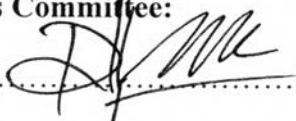
**Thesis Title:** Cellulose nanocomposite as an effective substrate for OLEDs  
**By:** Mr. Sarute Ummartyotin  
**Program:** Polymer Science  
**Thesis Advisors:** Asst. Prof. Hathaikarn Manuspiya  
Prof. Mohini Sain


---

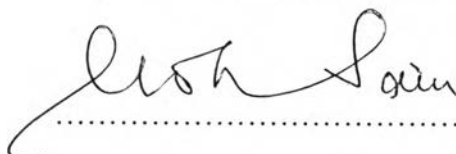
Accepted by the Petroleum and Petrochemical College, Chulalongkorn University, in partial fulfillment of the requirements for the Degree of Doctor of Philosophy


  
..... College Dean  
(Asst. Prof. Pomthong Malakul)

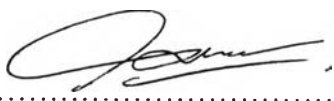
**Thesis Committee:**

  
.....  
(Asst. Prof. Pomthong Malakul)

  
.....  
(Asst. Prof. Hathaikarn Manuspiya)

  
.....  
(Prof. Mohini Sain)

  
.....  
(Assoc. Prof. Rathanawan Magaraphan)

  
.....  
(Dr. Adisorn Tuantranont)

## ABSTRACT

5292003063: POLYMER SCIENCE PROGRAM

Sarute Ummartyotin: Cellulose nanocomposite as an effective substrate for OLEDs

Thesis Advisors: Asst. Prof. Hathaikarn Manuspiya, Prof.

Mohini Sain 230 pp.

Keywords: cellulose nanocomposite / flexible display substrate / printed electronic / organic light emitting diodes

Nanocomposite film composed of bacterial cellulose (10 – 50 wt%) and polyurethane (PU) based resin was fabricated and utilized as a substrate for flexible organic light emitting diode (OLED) display. The performance of the nanocomposite satisfied the criteria for the substrate of OLED with an additional feature of flexibility. The visible light transmittance of the nanocomposite film was as high as 80 %. Its thermal stability was stable up to 150 °C while its dimensional stability in terms of coefficient of thermal expansion (CTE) was less than 20 ppm/K. Moreover, Si-O film and ferrofluid solution were employed to protect nanocomposite substrate from moisture and to reduce the surface roughness, respectively. Water vapor transmission rate (WVTR) and surface roughness must be lower than  $10^{-6}$  g/m<sup>2</sup>/day and 5 nm, respectively. Consequently, in order to fabricate OLED circuit, we investigated PEDOT: PSS, silver nanoparticle and ZnS nanoparticle were investigated for being as anode, cathode and emissive layer, respectively. The use of desktop inkjet printer was employed to use as instrument in order to deposit OLED layer.

## บทคัดย่อ

สรุป อำนวยการโยธิน : วัสดุคอมพอสิตของเซลลูโลส เพื่อนำมาเป็นแผ่นซับสเตรทของอุปกรณ์ไดโอดชนิดเปล่งแสง (Cellulose nanocomposite as an effective substrate for OLEDs) อ. ที่ปรึกษา: ผศ. ดร. ทักษกานต์ มนัสปิยะ และ ศ. ดร. โมหิณี เซน 185 หน้า

วัสดุคอมพอสิตสามารถเตรียมได้จากการเสริมแรงของเซลลูโลสเข้าสู่พอลิยูรีเทน ซึ่งสามารถเพิ่มในไปใช้เป็นแผ่นซับสเตรทในอุปกรณ์ไดโอดชนิดเปล่งแสง ซึ่งวัสดุดังกล่าวสามารถเพิ่มความยืดหยุ่น แสงสามารถผ่านได้เกิน 80 % นอกจากนี้ยังสามารถทนความร้อนได้ถึง 150°C และมีการขยายตัวทางความร้อนต่ำกว่า 20 ppm/K ต่อจากนั้นวัสดุคอมพอสิตดังกล่าว ยังถูกนำไปเคลือบด้วยฟิล์มของซิลิกอนออกไซด์ ซึ่งมีความหนาในระดับนาโน ด้วยกระบวนการเคลือบทางเคมี ซึ่งอาศัยพลาสมาเป็นตัวกระตุ้น เมื่อทำการเคลือบแล้ว พบว่า วัสดุคอมพอสิต สามารถลดการดูดซับน้ำได้ลดลงจาก 0.09 เหลือ  $10^{-4}$  g/m<sup>2</sup>/day นอกจากนี้ยังพบว่า วัสดุดังกล่าวยังคงให้ความโปร่งแสงได้เหมือนเดิม ต่อมาวัสดุคอมพอสิตที่ทำการเคลือบด้วยซิลิกอนออกไซด์ จะถูกนำมาขัดแบบละเอียดด้วยสารประกอบของเหล็ก ซึ่งมีขนาดเส้นผ่านศูนย์กลางประมาณ 30 นาโนเมตร เพื่อเป็นการลดระดับความสูงของพื้นผิวของชิ้นงานให้ต่ำกว่า 5 นาโนเมตร ซึ่งวัสดุดังกล่าวจะมีสมบัติโดยทั่วไปเหมือนแผ่นกระจก ซึ่งใช้กันแพร่หลายในแผ่นซับสเตรทของอุปกรณ์ไดโอดชนิดเปล่งแสง แต่ยังคงมีความยืดหยุ่นเหมือนแผ่นพลาสติก หลังจากนั้น จะเป็นการพัฒนาแผ่นซับสเตรทให้สอดคล้องกับอุตสาหกรรมผลิตวงจรรีเลย์ทรอนิกส์ด้วยเครื่องพิมพ์ โดยเริ่มจากการเตรียมขั้วแอโนดจากสาร PEDOT:PSS เพื่อทำหน้าที่ในการให้ประจุลบ ขั้วแคโทดจากสารละลายของเงินเพื่อให้ประจุบวก และสารที่ให้แสงจากสารประกอบซิงค์ซัลไฟด์เพื่อทำหน้าที่ให้แสง ซึ่งสารทั้ง 3 ประเภทนี้ จะต้องถูกปรับปรุงสมบัติทางกายภาพให้สอดคล้องกับเครื่องพิมพ์ สุดท้ายนี้ความสำเร็จดังกล่าว ยังเป็นการเพิ่มประสิทธิภาพของวัสดุชีวภาพในอุตสาหกรรมอิเล็กทรอนิกส์ด้วย

## ACKNOWLEDGEMENTS

The author would like to thank his supervisor, Assistant Professor Dr Hathaikarn Manuspiya, who gave him intensive recommendation, constructive criticism, suggestions, constant encouragement, inspiration, and the opportunity to study and have more experiences in The Petroleum and Petrochemical College, Chulalongkorn University, Thailand. Furthermore, he would like to express his appreciation to Center for Petroleum, Petrochemicals and Advanced Materials, Chulalongkorn University for financial support.

He is deeply indebted to Professor Dr Mohini Sain and Associate Professor Dr Amr Helmy who gave valuable advice and discussion on the research including a financial support during carrying out the experiments in Centre for Biocomposites and Biomaterials Processing, Faculty of Forestry, University of Toronto, Canada.

A deep gratitude is to express to Dr Julasak Juntaro, his postdoctoral researcher for the preparation of bacterial cellulose and its nanocomposite and long term mental support during period in Canada. The appreciation was also extended to Mr Natthaphon Bunnak for the CTE by dilatometer; trace metal element analysis by XRF and dielectric properties measurement by LCR precision meter at The Petroleum and Petrochemical College, Chulalongkorn University, Thailand.

He would like to thank all professors and friends at The Petroleum and Petrochemical College, Chulalongkorn University, Thailand and Faculty of Forestry, University of Toronto, Canada for giving him helps, good time and good memories during his stay.

Thus far, finally, he wishes to express his gratitude to his family for their love, understanding, encouragement, and for being a constant source of his inspiration.

## TABLE OF CONTENTS

	<b>PAGE</b>	
Title Page	i	
Abstract	ii	
Table of Contents	iii	
List of Tables	iv	
List of Figures	v	
<b>CHAPTER</b>		
<b>I</b>	<b>INTRODUCTION</b>	1
<b>II</b>	<b>OBJECTIVE AND HYPOTHESIS</b>	4
<b>III</b>	<b>LITERATURE REVIEW</b>	6
<b>IV</b>	<b>EXPERIMENTAL</b>	43
<b>V</b>	<b>DEVELOPMENT OF TRANSPARENT BACTERIAL CELLULOSE NANOCOMPOSITE FILM AS SUBSTRATE FOR FLEXIBLE ORGANIC LIGHT EMITTING DIODE (OLED) DISPLAY</b>	62
	5.1 Abstract	62
	5.2 Introduction	62
	5.3 Experimental	64
	5.4 Result and Discussion	65
	5.5 Conclusion	77
	5.6 Acknowledgement	78
	5.7 References	78
<b>VI</b>	<b>SI-O BARRIER TECHNOLOGY FOR</b>	

<b>CHAPTER</b>		<b>PAGE</b>
	<b>BACTERIAL CELLULOSE</b>	
	<b>NANOCOMPOSITE FLEXIBLE DISPLAYS</b>	82
	6.1 Abstract	82
	6.2 Introduction	82
	6.3 Experimental	84
	6.4 Result and Discussion	86
	6.5 Conclusion	100
	6.6 Acknowledgment	100
	6.7 References	100
<b>VII</b>	<b>THE ROLE OF FERROFLUID ON SURFACE</b>	
	<b>SMOOTHNESS OF BACTERIAL</b>	
	<b>CELLULOSE NANOCOMPOSITE DISPLAY</b>	105
	7.1 Abstract	105
	7.2 Introduction	105
	7.3 Experimental	106
	7.4 Result and Discussion	110
	7.5 Conclusion	117
	7.6 Acknowledgement	117
	7.7 References	117
<b>VIII</b>	<b>DEPOSITION OF PEDOT:PSS</b>	
	<b>NANOPARTICLES AS A CONDUCTIVE</b>	
	<b>MICRO-LAYER ANODE IN OLEDs DEVICE</b>	
	<b>BY DESKTOP INKJET PRINTER</b>	121
	8.1 Abstract	121
	8.2 Introduction	121
	8.3 Experimental	123
	8.4 Result and Discussion	126

<b>CHAPTER</b>		<b>PAGE</b>
	8.5 Conclusion	134
	8.6 Acknowledgement	134
	8.7 References	134
<b>IX</b>	<b>SYNTHESIS OF COLLOIDAL SILVER NANOPARTICLE FOR PRINTED ELECTRONIC</b>	140
	9.1 Abstract	140
	9.2 Introduction	140
	9.3 Experimental	142
	9.4 Result and Discussion	144
	9.5 Conclusion	152
	9.6 Acknowledgement	152
	9.7 References	152
<b>X</b>	<b>SYNTHESIS AND LUMINESCENCE PROPERTIES OF ZNS AND METAL (MN,CU)-DOPED-ZNS CERAMIC POWDER</b>	155
	10.1 Abstract	155
	10.2 Introduction	155
	10.3 Experimental	156
	10.4 Result and Discussion	159
	10.5 Conclusion	169
	10.6 Acknowledgement	170
	10.7 References	170
<b>XI</b>	<b>HYBRID ORGANIC-INORGANIC OF ZNS</b>	



<b>EMBEDDED PVP NANOCOMPOSITE FILM FOR PHOTOLUMINESCENT APPLICATION</b>	174
11.1 Abstract	174
11.2 Introduction	174
11.3 Experimental	175
11.4 Result and Discussion	178
11.5 Conclusion	184
11.6 Acknowledgement	184
11.7 References	185
<b>CONCLUSIONS AND RECOMMENDATION</b>	188
<b>REFERENCES</b>	190
<b>CURRICULUM VITAE</b>	211

## LIST OF TABLES

<b>TABLE</b>		<b>PAGE</b>
<b>CHAPTER III</b>		
3.1	Composition and comparative properties of natural and man-made fibers	7
3.2	A classification of the bacteria's capability to produce cellulose	8
3.3	Properties of bacterial cellulose	13
3.4	The basic properties of OLED materials	25
<b>CHAPTER V</b>		
5.1	Thermal and optical properties of bacterial cellulose, neat PU resin, and nanocomposite	70
<b>CHAPTER VI</b>		
6.1	WTVR properties of the nanocomposites in comparison to the OLED requirement and conventional polymers	97
<b>CHAPTER VII</b>		
7.1	Formulation of magnetic compound fluid (MCF)	108
<b>CHAPTER VIII</b>		
8.1	Contact angle, viscosity, surface tension and conductivity of PEDOT: PSS Ink formulation	127
8.2	The numbers of layer and film thickness measured by profilometer	129

<b>TABLE</b>		<b>PAGE</b>
8.3	The relationship of numbers of layer and resistivity and conductivity	130
<b>CHAPTER X</b>		
10.1	Crystallite size and lattice parameter of ZnS, and ZnS doped with Cu and Mn	163
10.2	XRF quantitative analysis of ZnS and metal-doped ZnS ceramic	165

## LIST OF FIGURES

FIGURE	CHAPTER III	PAGE
3.1	Chemical structure of cellulose	6
3.2	Scheme for the formation of bacterial cellulose. Reproduced from Jonas and Farah	12
3.3	Proposed biochemical pathway for cellulose synthesis in <i>Acetobacter xylinum</i> . Reproduced from Cannon and Anderson	13
3.4	Renewability and Biodegradability cycle of bacterial cellulose	14
3.5	Deformable sheet with embedded bacterial cellulose: the lines show deformation of the sheet when stretched. Reproduced from Bunsell and Renard	17
3.6	Solid particles layout in forming a cell inside the porous layer	19
3.7	Representative volume elements in composite	20
3.8	SEM of fracture surfaces of epoxy composites based on long viscous fibers (a) without treatment (b) after treatment with silane	22
3.9	OLED structures. The total organic thin film thickness is typically ~ 100 nm.	24
3.10	Structure of some molecular semiconductors that have been used in OLEDs. Alq is used as an electron transport and emissive layer, TPD or NPB is used as a hole transport layer	25
3.11	Schematic energy level diagram of OLEDs under forward bias	26

<b>FIGURE</b>		<b>PAGE</b>
3.12	OLED working principles, $J_h'$ , $J_e'$ stand for leakage current in ETL and HTL respectively	27
3.13	Measured $\mu$ vs T for three $\alpha$ -6T TFT' A, B and C	31
3.14	Variation of the hole mobility of a 6T poly-crystalline film as a function of gate bias. Data were recorded at 300K. Closed circles correspond to uncorrected data, and open circles to data corrected for the contact series resistance	31
3.15	Electroluminescence spectra at normal directions in ITO/TPD (50 nm)/Alq/MgAg devices	34
3.16	Schematic layer structure of a patterned planar microcavity in which the $Si_3N_4$ filler layer is etched to three different thicknesses to change the optical properties	35
3.17	Electroluminescence spectrums from a three-mode microcavity LED, in which the three peaks are at 488, 543, and 610 nm	35
3.18	Market prospect for flexible displays	37
3.19	Potential candidate polymers for flexible display substrate	38
3.20	Glass transition temperature ( $T_g$ ) of commercially available polymer	39
3.21	Cross-sectional structure of flexible displays	41
3.22	Requirement of WVTR and OTR for electronic devices	42

## CHAPTER V

5.1	Optical transparency of bacterial cellulose nanocomposite film and bacterial cellulose sheet	66
5.2	Refractive indices of neat PU based resin and bacterial cellulose nanocomposite as a function of wavelength	67
5.3	AFM investigation of (A) bacterial cellulose sheet and	

<b>FIGURE</b>	<b>PAGE</b>
	69
5.4	71
5.5	72
5.6	73
5.7	75
5.8	76
5.9	77

## CHAPTER VI

6.1	87
6.2	88
6.3	89
6.4	90
6.5	91
6.6	93
6.7	94

<b>FIGURE</b>		<b>PAGE</b>
6.8	Typical FCP of ~100 nm-thick Si-O barrier deposited on cellulose nanocomposite substrate in ambient air	95
6.9	WVTR of ~100 nm-thick Si-O deposited on cellulose nanocomposite substrate versus deposition chamber pressure	98
6.10	WVTR of ~100 nm-thick Si-O deposited on cellulose nanocomposite substrate versus RF power	99

#### CHAPTER VII

7.1	Schematic drawing of processing principle	108
7.2	XRD pattern of ferrofluid nanoparticle in solid state	111
7.3	TEM investigation of ferrofluid solid nanoparticle (A) magnification 50000X (B) magnification 100000X	112
7.4	Histogram of magnetic nanoparticle in aqueous solution	113
7.5	Shear stress versus shear rate of ferrofluid	113
7.6	Shear thinning behavior of the ferrofluid	114
7.7	Top view AFM image of polishing condition A	115
7.8	Top view AFM image of (A) Non-polishing (B) Polishing with ferrofluid condition A (C) Polishing with ferrofluid condition B	116

#### CHAPTER VIII

8.1	TEM image of PEDOT: PSS nano-particle in aqueous solution	126
8.2	Schematic diagram of test circuit for measuring bar specimen resistivity with the four-point probe method	130
8.3	The linear relationship between number of layer and conductivity value	131
8.4	The photograph of PEDOT: PSS as anode by Desktop	

<b>FIGURE</b>		<b>PAGE</b>
	inkjet printer	132
8.5	AFM investigation of PEDOT: PSS coated on resin in (a) 3 and (b) 5 layers, respectively	133

#### CHAPTER IX

9.1	Illustration of direct chemical synthetic route of silver nanoparticle from the reaction of silver nitrate and PVP solution	143
9.2	FTIR spectra of pure silver, PVP solution, mixture of pure silver nanoparticle and PVP solution	146
9.3	Transmission electron microscope of silver nanoparticle (A) silver nanoparticle prepared from PVP (Mw~40000) (B) silver nanoparticle prepared from PVP (Mw~10000) at 60000 X magnifications	147
9.4	Transmission electron microscope of silver nanoparticle prepared from PVP (Mw~40000) at 150000X magnification	148
9.5	X-ray diffraction of silver nanoparticle	148
9.6	Schematic drawing of ideal arrangement of small and large particles in printed silver lines particles in printed silver lines	150
9.7	SEM image of silver nanoparticle	150
9.8	Current density ( $J/cm^2$ ) vs Applied voltage (V) for synthesis of silver thin film	151

#### CHAPTER X

10.1	FTIR spectra of ZnS, and Mn doped ZnS, Cu doped ZnS and Mn-Cu codoped ZnS	160
10.2	XRD pattern of ZnS, and metal (Mn, Cu)-doped-ZnS	162



<b>FIGURE</b>		<b>PAGE</b>
10.3	Field emission scanning electron microscope (FESEM) and energy dispersion analysis (A) ZnS (B) Mn-doped-ZnS (C) Cu-doped-ZnS (D) Mn-Cu-codoped-ZnS	164
10.4	The fluorescence image of ZnS particle without excitation and the fluorescence image of ZnS particle with excitation (A) ZnS (B) Mn-doped-ZnS (C) Cu-doped-ZnS (D) Mn-Cu-codoped-ZnS	166
10.5	Photoluminescence spectra of ZnS and metal-doped ZnS particle (A) ZnS (B) Mn-doped-ZnS (C) Cu-doped-ZnS (D) Mn-Cu-codoped-ZnS	168
10.6	Energy level of ZnS, Mn-doped ZnS and Cu-doped ZnS	169
 CHAPTER XI  		
11.1	FTIR spectra of ZnS/PVP solution and ZnS/PVP hybrid nanocomposite film	179
11.2	XRD spectra of neat PVP film, ZnS embedded PVP film and bulk ZnS particle	180
11.3	TEM and SEM image of ZnS nanoparticle	181
11.4	SEM image of printed hybrid organic-inorganic ZnS embedded PVP film	182
11.5	Photoluminescent image of ZnS embedded nanocomposite (A) without excitation (B) with excitation	183
11.6	PL spectra of ZnS embedded PVP hybrid nanocomposite	184